

2-(o-Hydroxyphenyl)Benzimidazole as a New Corrosion Inhibitor for mild Steel in Hydrochloric Acid Solution

Y. Abboud^{1,2}, B. Hammouti^{3,*}, A. Abourriche^{1,2}, B. Ihssane¹, A. Bennamara¹, M. Charrouf¹, S.S Al-Deyab⁴

¹ Laboratoire de Biomolécule et Synthèse Organique, Faculté des Sciences Ben M'sik, Casablanca, Morocco.

² Centre d'Analyse et de Recherche, Faculté des Sciences Ben M'sik, Casablanca, Morocco.

³ Laboratoire de Chimie Appliquée et environnement, Faculté des Sciences, Oujda, Morocco.

⁵ Petrochemical Research Chair, Department of Chemistry, College of Science, King Saud University, B.O. 2455, Riaydh 11451, Saudi Arabia

*E-mail: hammoutib@gmail.com

Received: 29 January 2012 / Accepted: 17 February 2012 / Published: 1 March 2012

In this study, 2-(o-Hydroxyphenyl)benzimidazole (HPB) was synthesized, characterized and tested as a new corrosion inhibitor for mild steel in 1M HCl solution. Weight-loss, Spectrophotometric and potentiodynamic polarization measurements were applied to analyse the metal corrosion behaviour in the absence and presence of different concentrations of the inhibitor. Results obtained revealed that this compound has fairly good inhibiting properties for mild steel corrosion in 1M HCl solution, with efficiency of around 93 % at a concentration of 500 μ M. The inhibition was of a mixed anodic-cathodic nature with predominance of anodic character. The film which is formed over the metal surface was analysed by FT-IR spectroscopy. Further examination using X-ray diffraction confirms the role of HPB as an effective corrosion inhibitor for mild steel in acid media.

Keywords: Corrosion; inhibitor; mild steel; acidic media; Hydroxyphenyl-benzimidazole

1. INTRODUCTION

The inhibition of steel corrosion by hydrochloric acid was previously studied using some nitrogen and oxygen containing organic compounds [1-8]. These compounds adsorb on the steel surface and block the active sites on the surface and thereby reduce the corrosion rate. Generally, inhibition efficiency of organic compounds always increases with the number of aromatic systems and electronic availability in the molecule. Granese et al. [9] have studied the interactions of the n-

hexadecyl derivatives of pyridine, quinoline and acridine inhibitors with Fe and steel surfaces in HCl media and reported that the strongest being observed with the acridine derivatives, whereas the weakest ones appeared to occur with the pyridine derivatives. Ajmal et al. [10] have studied the effect of 2-hydrazino-6-methylbenzothiazole on the corrosion of steel in 1M HCl and 1M H₂SO₄ and reported that the presence of an aromatic ring and functional groups containing nitrogen and oxygen are likely to induce a greater adsorption of the compounds on the metal surface promoting effective inhibition.

Benzimidazole and phenol derivatives are commonly employed as corrosion inhibitors for protecting steel and have been the subject of several investigations. The roles of the individual functional groups in the inhibition mechanism have been widely reported [11-25]. However, to the best of our knowledge, no study has examined the effect of having the two functional groups in one molecule. Accordingly, the present work reports the use of 2-(*o*-Hydroxyphenyl) benzimidazole which have the particularity to possess both benzimidazole and phenol parts as corrosion inhibitor for steel in 1M HCl.

2. EXPERIMENTAL

2.1. Synthesis of 2-(*o*-Hydroxyphenyl) benzimidazole

2-(*o*-Hydroxyphenyl) benzimidazole was prepared by coupling salicylaldehyde with 1,2-phenylenediamine according to the method of Q. Shi et al. [26] and was purified and characterised by NMR and IR spectroscopies before use. Fig.1 shows the molecular structure of the investigated compound which has been labelled (HPB).

2.2. Metal specimen

Corrosion tests were performed on a mild steel of the following percentage composition (weight per cent): 0.21C, 0.38Si, 0.09P, 0.05Mn, 0.05S, 0.01Al and the remainder iron.

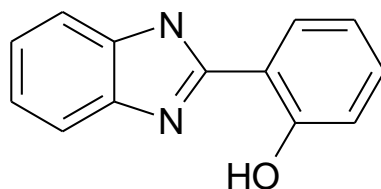


Figure 1. Chemical structure of (HPB)

2.3. Aggressive solution

The aggressive solution used was made of AR grade 37 % HCl. A 1M solution of the acid was prepared using bidistilled water. The concentration range of the inhibitor employed was 10 μM to 500 μM , in 1M HCl.

2.4. Weight loss measurements

Gravimetric measurements were carried out in double walled glass cell equipped with a thermostatic cooling condenser. The solution volume was 100 cm^3 , the temperature was 25 ± 1 $^\circ\text{C}$ and the immersion time was 6 h. Each experiment was repeated at least three times to ensure reproducibility and average weight loss was noted. The inhibition efficiency (%) was determined by following equation:

$$E (\%) = \frac{W_0 - W}{W_0} \times 100 \quad (1)$$

Where W ($\text{mg cm}^{-2} \text{ h}^{-1}$) and W_0 ($\text{mg cm}^{-2} \text{ h}^{-1}$) are the values of corrosion rates of mild steel without and with inhibitor.

2.5. Potentiodynamic polarisation measurements

Polarisation experiments were carried out in a conventional three-electrode cell with a platinum counter electrode (CE) and saturated calomel electrode (SCE) as the reference electrode. The working electrode (WE) was in the form of a disc cut from mild steel with exposed surface area 1cm^2 . The freshly polished electrode was immersed in test solution at open circuit potential until a steady state was reached. All polarisation curves were recorded with Amel potentiostat (model 2053) from cathodic potential of -0.250 V vs. SCE to an anodic potential of $+0.250$ V vs. SCE with respect to the open circuit potential at a sweep rate 20mVmn^{-1} in aerated condition and temperature thermostatically controlled at 25 ± 1 $^\circ\text{C}$ to make the conditions identical to weight loss measurements. The corrosion inhibition efficiency E (%) was evaluated from the measured (I_{corr}) values obtained by extrapolation of cathodic and anodic Tafel lines to (E_{corr}) using the relationship:

$$E (\%) = \frac{I_{\text{corr}} - I_{\text{corr}}^{\text{inh}}}{I_{\text{corr}}} \times 100 \quad (2)$$

Where I_{corr} and $I_{\text{corr}}^{\text{inh}}$ are the corrosion current densities without and with the addition of various concentration of the inhibitor.

2.6. Atomic absorption spectrophotometric studies

The amount of iron dissolved from both unprotected and protected samples was determined by using a fully automated, computer-controlled atomic absorption spectrometer (model 908; GBC-Australia), and using air-acetylene flame. Three independent probes with a blank probe were analysed for each of the samples examined. From the amount of dissolved iron, the inhibition efficiency values E (%), were calculated as follows:

$$E (\%) = \frac{C_0 - C}{C_0} \times 100 \quad (3)$$

Where C_0 (mg l^{-1}) and C (mg l^{-1}) are iron concentration after immersion in solution without and with inhibitor.

2.7. Surface examinations

The nature of the film formed on the surface on the metal specimens was analysed by FT-IR and XRD. The infrared spectrum was obtained as KBr pellets on a Bruker Tensor-27 spectrophotometer while the corrosion products were identified by X-Ray diffraction (model: XRD-Bruker D8 Advance).

3. RESULTS AND DISCUSSION

3.1. Weight loss and spectrophotometric measurements.

The results obtained for both weight loss measurement and atomic absorption spectroscopy (Table 1) indicates that the mild steel corrosion is reduced by the presence of HPB in 1M HCl at all concentrations used in this study, since there is a general decrease in the original weight of mild steel and in the amount of dissolved iron at the end of the corrosion monitoring process. This may be ascribed to the adsorption of this compound on the mild steel surface, producing a barrier, which isolates the surface from the corrosion environment.

It has also been observed that the corrosion rate and the rate of steel dissolution decrease gradually with increasing inhibitor concentration and the degree of inhibition depends on the concentration of HPB.

The inhibition efficiency was estimated to be 82% even at extremely low concentration (10 μM) and reaches 94% at a concentration of (500 μM). Such remarkable performances may be due to, the high molecular weight of HPB, the presence of C=N, O-H which are electron donation groups and the presence of aryl groups.

Table1. Inhibition efficiency of different concentrations of HPB for the corrosion of mild steel in 1M HCl at 298K obtained from weight loss measurement and atomic absorption spectroscopy

Inhibitor concentration (μM)	W corr (mg h-1cm-2)	Amount of dissolved iron ($\mu\text{g l-1}$)	E (%) weight loss	E (%) atomic absorption spectroscopy
Blank	0.742	0.128	—	—
10	0.132	0.021	82.2	83.6
50	0.092	0.016	87.6	87.5
100	0.066	0.012	91.1	90.6
500	0.042	0.009	94.3	92.9

3.2. Electrochemical measurements

Fig.2 shows the cathodic and anodic polarization curves of mild steel in 1M HCl solution without and with different concentrations of HPB at 298 K. Values of all electrochemical parameters such as corrosion potential (E_{corr}), cathodic and anodic Tafel slopes (b_c , b_a) and corrosion current density (I_{corr}) attained by extrapolation of Tafel lines, as well as inhibitor efficiency are listed in Table 2.

From Fig. 2, it is clear that the values of (I_{corr}) of mild steel in the inhibited solution were smaller than those for the inhibitor-free solution. The addition of HPB induces a decrease in both cathodic and anodic currents. This result shows that the addition of HPB hindered the acid attack on the steel electrode.

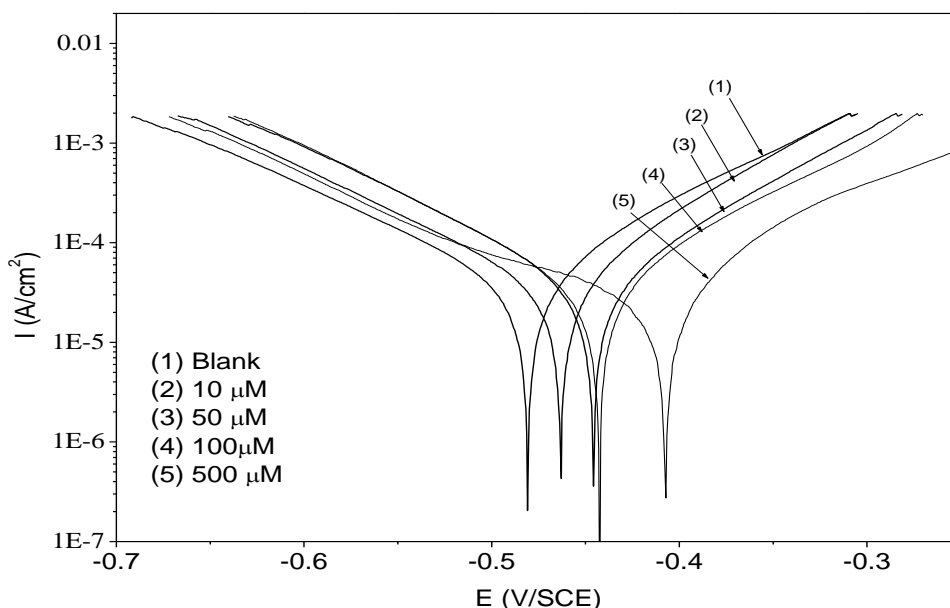


Figure 2. Polarization curves for mild steel in 1M HCl without and with different concentration of HPB.

Table 2. Electrochemical parameters for mild steel in absence and presence of different concentrations of HPB at 298°C obtained from Tafel extrapolation

C (μ M)	E_{corr} (mV/SCE)	b_c (mV/dec)	b_a (mV/dec)	I_{corr} (μ A/cm ²)	E %
Blank	-480	-121	89	277	—
10	-463	-113	85	43	84.5
50	-445	-112	88	38	86.3
100	-442	-108	90	29	89.5
500	-407	-119	84	21	92.4

Further inspection of Fig.2 reveals that in the cathodic range, the cathodic currents densities were less sensitive to HPB concentration while in the anodic range, a significant decrease in the anodic current densities lead to a shift of the corrosion potentials (E_{corr}) toward more positive direction are noted when the inhibitor concentration increased. Therefore, It could be concluded that this compound can be classified as a mixed type inhibitor but dominantly act as an anodic inhibitor for mild steel in 1M HCl. It is also noticed as can be seen from of Table 2 that the presence of different concentration of HPB did not change significantly the cathodic and anodic Tafel slope values (b_c , b_a) relative to the blank. This finding would indicate that the inhibition effect is caused by blocking of metal surface electrode by adsorbed inhibiting species without affecting the anodic and cathodic reaction mechanism.

3.3. FTIR studies

The mode of bonding of the HPB to metal surface was elucidated by comparing the IR spectrum of the pure compound with the spectrum of the film formed on the surface of the metal specimen after a potentiodynamic polarization experiment carried out in 1 M HCl in the presence of 500 μ M HPB.

The infrared spectrum of HPB (Fig.3A) indicates the presence of phenolic oxygen band and the characteristic bands due to benzimidazole nucleus: C=C aromatic groups, NH imine group and CN pyridil group.

The bands at 3438 cm^{-1} and 3325 cm^{-1} are due to $\nu(\text{O-H})$ and $\nu(\text{N-H})$ stretching vibration frequencies, respectively.

These bands appear closer to each other due to intramolecular hydrogen bonding between the phenoxy hydrogen atom and one of the imine nitrogen atoms. The $\nu(\text{C=C})$ frequencies for the benzimidazole and phenol rings are expected to appear at 1496 cm^{-1} . Similarly the $\nu(\text{C=N})$ and the characteristic $\nu(\text{C-H})$ and $\delta(\text{C-H})$ modes of ring residues were observed in 1627, 3055 and 727 cm^{-1} , respectively.

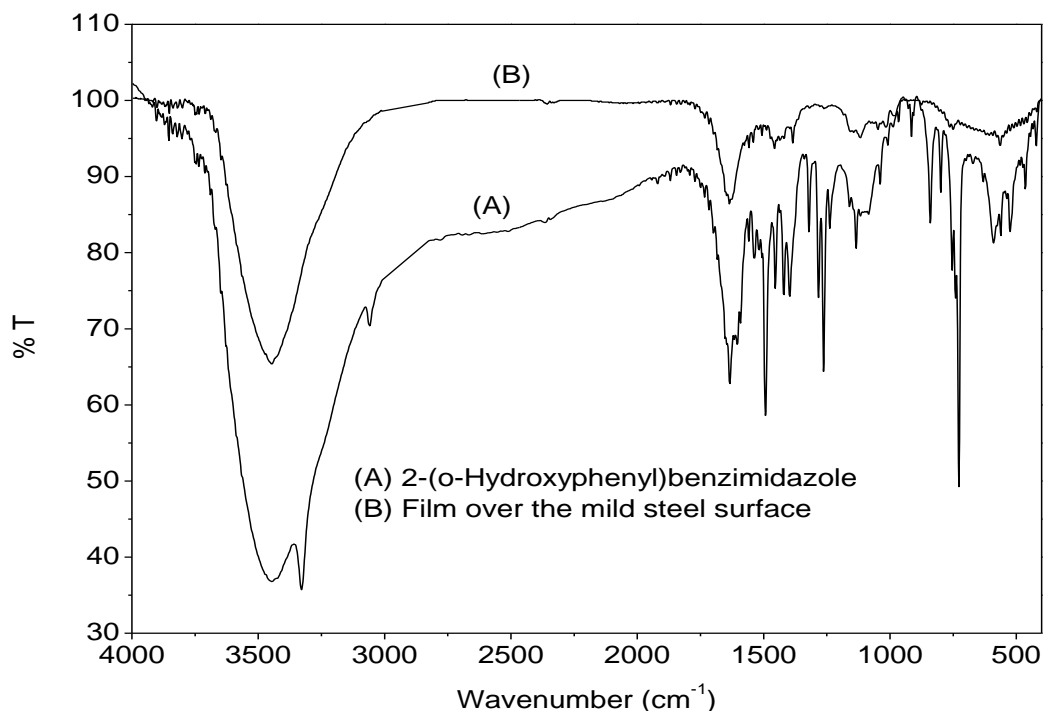


Figure 3. IR absorption spectra of HPB and the film formed over inhibited mild steel sample

By comparing the spectrum of adsorbed film (Fig.3B) with that of HPB, we can conclude that the two spectra are similar in their spectral features. The presence of bands around 3452 and 1637 cm^{-1} characteristics to O-H and C=N stretching vibration frequencies confirm the presence of HPB or at least, its complex with iron in the formed film. The disappearance of N-H stretching vibration from (3300 to 3000 cm^{-1}) and the slight shift in O-H and C=N stretching bands to higher wavenumbers clearly proved that these electron centers are involved in the sharing of electron with metal. These changes may support the argument that the imine nitrogen and phenolic oxygen atoms are coordinated with Fe^{2+} . HPB may be adsorbed on the steel surface and rapidly react with iron cations on/or around the surface to form $[\text{HPB-Fe}^{2+}]$ complexes on the steel surface. The presence of HPB over the complex surface was evidenced by the characteristics bands for O-H and C=N. Furthermore, the intensity of these stretching frequency is decreased which implies that HPB is coordinated to Fe^{2+} resulting in the formation of a Fe^{2+} - inhibitor complex on the metal surface. Imidazole derivatives are known in literature to exhibit good and excellent inhibitory effect according to the molecular structure. 2-Mercapto-1-methylimidazole is an efficient corrosion inhibitor of copper in aerated 3% NaCl solution [27]. The addition of 2-mercapto benzimidazole (2MBI) on mild steel in 1.0 M hydrochloric acid led to 98% at 10^{-3}M [12].

3.4. X-ray diffraction analysis

The X-ray diffraction patterns of the surface of the mild steel specimens immersed in various test solutions are given in Fig.4. Peaks at $2\theta = 30^\circ$, 35.4° , 42.9° and 64.9° can be assigned to oxides of

iron. The peaks due to iron appear at $2\theta = 44.6^\circ$, 82.3° and 92.8° . Thus, it is observed that in absence of inhibitor (Fig. 4A), the surface of the metal contains iron oxides of Fe_3O_4 and FeOOH . The XDR patterns of inhibited surface (Fig.4B) show the presence of iron peaks only, the peaks due to oxides of iron are found to be absent. The formation of adsorbed protective film on the surface of metal in the presence of OPB is clearly reflected from these observations. This method may be useful to complete interaction of organic inhibitor with metallic surface [28].

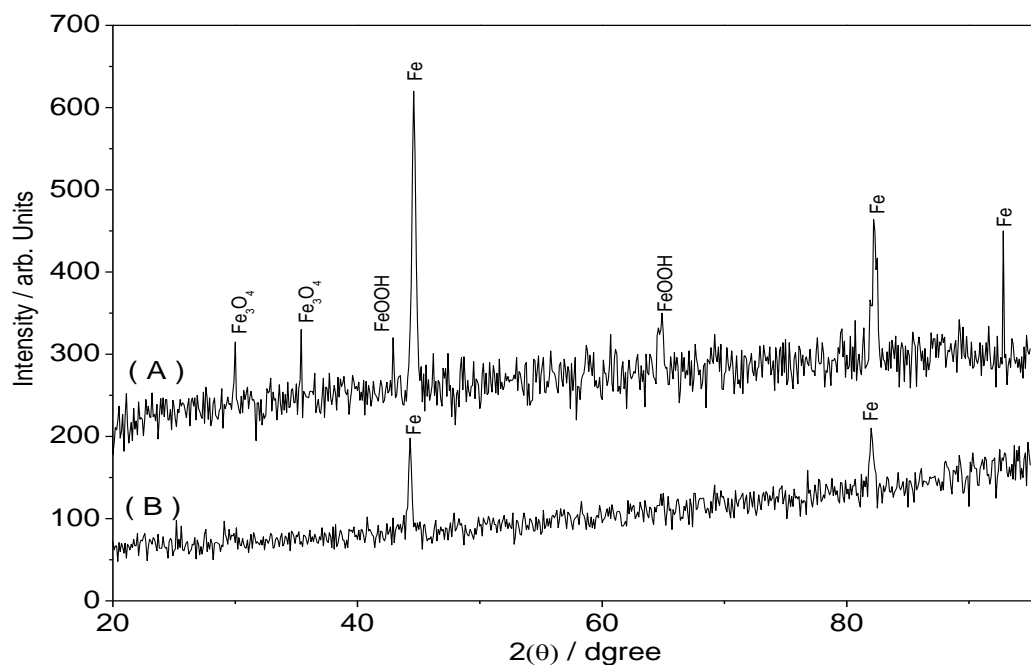


Figure 4. XDR pattern of the surface film formed on mild steel after immersion in 1M HCl (A) without (B) with 500 μM HPB.

4. CONCLUSION

From the results it is evident that HPB shows excellent inhibition properties for the corrosion of mild steel in 1 M HCl at 298K, and the inhibition efficiency increases with increase in the inhibitor concentration. The inhibitor efficiencies determined by weight loss, atomic absorption spectrophotometry and Tafel polarization methods are in reasonable agreement. Based on the Tafel polarization results, HPB can be classified as mixed inhibitor with predominance of anodic character. Surface analysis reveals the formation of complex between HPB and metal surface.

ACKNOWLEDGEMENTS

Prof S. S. Al-Deyab and Prof B. Hammouti extend their appreciation to the Deanship of Scientific Research at King Saud University for funding the work through the research group project.

References

1. I. Ahamad, R. Prasad, M.A. Quraishi, *Corros Sci.* 52 (2010) 3033-3041.
2. P. Lowmunkhong, D. Ungthararak, P. Sutthivaiyakit, *Corros Sci* 52 (2010) 30-36.
3. F.S. de Souza, A. Spinelli, *Corros Sci* 51 (2009) 642-649
4. Y. Abboud, A. Abourriche, T. Saffaj, M. Berrada, M. Charrouf, A. Bennamara, H. Hannache, *Desalination* 237 (2009) 175-189.
5. X. Li, S. Deng, H. Fu, *Corros Sci* 52 (2010) 3413-3420.
6. A. Ostovari, S.M. Hoseinie, M. Peikari, S.R. Shadizadeh, S.J. Hashemi, *Corros Sci* 51 (2009) 1935-1949.
7. Y. Abboud, A. Abourriche, T. Saffaj, M. Berrada, M. Charrouf, A. Bennamara, N. Al Himidi, H. Hannache, *Mater Chem Phys* 105 (2007) 1-5.
8. S. Vishwanatham, N. Halder, *Corros Sci* 50 (2008) 2999-3004.
9. S.L. Granese, B.M. Rosales, C. Oviedo, J.O. Zerbino, *Corros Sci* 33 (1992) 1439-1453.
10. M. Ajmal, A.S. Mideen, M.A. Quraishi, *Corros Sci* 36 (1994) 79-84.
11. M. Abreu-Quijano, M. Palomar-Pardavé, A. Cuán, M. Romero-Romo, G. Negrón-Silva, R. Álvarez-Bustamante, A. Ramírez-López, H. Herrera-Hernández, *Int. J. Electrochem. Sci.*, 6 (2011) 3729-3742
12. M. Benabdellahn A. Tounsi, K.F. Khaled, B. Hammouti, *Arabian J. Chem.* 4 (2011) 17-24.
13. I. Ahamad, M.A. Quraishi, *Corros Sci* 51 (2009) 2006-2013.
14. K.F. Khaled, *Electrochim Acta*, 48 (2003) 2493-2503.
15. S. Muralidharan, S. Venkatakrishna Iyer, *Anti-Corros Methods Mater* 44 (1997) 100-106.
16. Y. Abboud, A. Abourriche, T. Saffaj, M. Berrada, M. Charrouf, A. Bennamara, A. Cherquaoui, D. Takky, *Appl Surf Sci* 252 (2006) 8178-8184.
17. A. Dafali, B. Hammouti, S. Kertit, *J. Electrochem. Soc. Ind.* 50 (2001) 62-67.
18. A. Popova, *Corros Sci* 49 (2007) 2144-2158.
19. Y. Abboud, B. Ihssane, B. Hammouti, A. Abourriche, S. Maoufoud, T. Saffaj, M. Berrada, M. Charrouf, A. Bennamara, H. Hannache, *Desalination and Water Treatment*, 20 (2010) 35-44.
20. A. Dafali, B. Hammouti, A. Aouniti, R. Mokhlisse, S. Kertit, K. Elkacemi, *Ann. chim. Sci. Mat.*, 25 (2000) 437-446.
21. S. Rengamani, S. Muralidharan, M. Anbu Kulandainathan, S. Venkatakrishna Iyer, *J. Appl. Electrochem.* 24 (1994) 355-360.
22. F.S. De Souza, A. Spinelli, *Corros Sci* 51 (2009) 642-649.
23. K. Bouhrira, F. Ouahiba, D. Zerouali, B. Hammouti, M. Zertoubi, N. Benchat, *E-Journal of Chemistry*, 7 (2010) S35-S42.
24. A.Y. El-Etre, *J Colloid Interface Sci* 314 (2007) 583.
25. M. Benabdellah, A. Ousslim, B. Hammouti, A. Elidrissi, A. Aouniti, A. Dafali, K. Bekkouch, M. Benkaddour, *J. Appl. Electrochem.* 37 (2007) 819-826.
26. Q. Shi, S. Zhang, F. Chang, P. Hao, W.H. Sun, *Comptes Rendus Chimie* 10 (2007) 1200-1208.
27. A. Dafali, B. Hammouti, A. Aouniti, R. Mokhlisse, S. Kertit, K. Elkacemi, *Annales de Chimie Science des Matériaux*, 25 (2000) 437.
28. Y. Abboud, B. Hammouti, A. Abourriche, A. Bennamara, H. Hannache, *Research on Chemical Intermediates*, (2012), DOI: 10.1007/s11164-012-0486-0